Electronic Supplementary Information

Programmable Motion Control and Trajectory Manipulation of Microparticles Through Tri-Directional Symmetrical Acoustic Tweezers

Yancheng Wang[a*], Hemin Pan[b], Deqing Mei[a], Chengyao Xu[b] and Wanyu Weng[b]

[a.] *State Key Laboratory of Fluid Power and Mechatronic Systems, School of Mechanical Engineering, Zhejiang University, Hangzhou 310027, China.*

[b.] *Key Laboratory of Advanced Manufacturing Technology of Zhejiang Province, School of Mechanical Engineering, Zhejiang University, Hangzhou 310027, China*

**Corresponding author: Yancheng Wang*

E-mail: yanchwang@zju.edu.cn; Tel.: (+86) 571-87951906; Fax: (+86) 571-87951145

Supplementary Materials

The PDF file includes:

Notes S1 to S3

Fig. S1 to S8

Table S1

Legends for Movies S1 to S11

References

Other Supplementary Materials for this manuscript includes the following:

Movies S1 to S11

Note S1: Boundary condition settings of numerical model

Figs. S1a, b illustrate the final meshing result of the developed 3D numerical model. It includes a $LiNbO_3$ substrate layer, IDTs layer, and liquid layer. A circular-shaped liquid layer is utilized and placed on the $LiNbO_3$ substrate layer; two sets of IDTs are evenly distributed around the liquid layer. Fig. S1c demonstrates the boundary conditions for the established 3D FEM model. A fixed constraint boundary (BC_{fix}) is added at the bottom of the Z-cut $LiNbO_3$ substrate layer. In addition, setting a low-reflecting boundary condition (BC_{low}) on the outside of the Z-cut $LiNbO_3$ substrate layer enables stable transmission of TSAWs over the substrate layer without apparent reflected waves. Then the boundary conditions of ground (BC_{gro}) and electric potential (BC_{pot}) are added to the IDTs alternately. The electric potential conditions are set to 10 V, and the ground conditions are set to 0 V, respectively. And the frequencies are set at 10.5-11.1 MHz for the IDTs. Finally, the surface of the liquid layer is set as an impedance boundary to replace the annular PDMS chamber.

Note S2: Approximate substitute for the time-averaged acoustic pressure field

We consider using the instantaneous pressure field when the transmission of the acoustic waves has stabilized to predict the moving trend of the particles throughout the migration process. The time-domain finite element model (FEM) uses an explicit calculation method, which outputs a discrete solution in time step. The time-averaged calculation of the acoustic pressure p achieved entirely in one period requires the preservation of a large number of outputs. Since the excitation frequency of the interdigital electrodes (IDTs) is equal to the resonance frequency of the Z-cut lithium niobate ($LiNbO_3$) substrate, the acoustic pressure p can therefore be estimated as

$$p_{\text{avgi}}(x,y,z,t) = p(x,y,z)e^{i(\omega_1 t+\pi)} \tag{S1}$$

Substituting equation S1 into into the calculation of FARF can have

$$F_{ARF} \propto \left\langle p_{\text{avgi}}^2(x,y,z,t)\Big|_{t=n\frac{T}{2}} \right\rangle \tag{S2}$$

Equation S2 shows that the acoustic radiation force excited by TSAWs can be expressed by the acoustic pressure at a fixed time point, and the calculation reference points are shown in Fig. S2. This avoids integration operations in one period and significantly reduces the computational effort.

When several IDTs are excited simultaneously, their calculation reference points are always the same because of the same frequency of their input electrical signals. This allows excitation signals generated by different IDTs to reach maximums at the same time. In addition, because of the low power of TSAWs, the acoustic excitation does not impact the properties of $LiNbO_3$, so it can be assumed that the acoustic pressure satisfies superposition principles. When multiple IDTs work simultaneously, the acoustic pressure excitation can be considered as the superposition of the acoustic pressure with each IDT working individually. The superimposed acoustic pressure can be calculated as

$$p_{\mathrm{avgN}}(x,y,z,t)=\sum_{i=1}^{N}p_{\mathrm{avgi}}(x,y,z)e^{i(\omega_1 t+\pi)} \tag{S3}$$

In summary, equation S3 can be used to calculate the time-averaged stable distribution of the acoustic pressure field within the chamber by using the acoustic pressure at a point in time after the model has converged. It effectively saves complex integration over a period of time without computational accuracy loss. Therefore, after consideration, we chose to use the instantaneous acoustic pressure field at a specific time point as an approximate substitute for the time-averaged acoustic pressure field.

Note S3: Determination of IDTs' geometric parameters

The main parameters of the IDT include the pair number of the fork fingers (N), the acoustic aperture (W), and the electrode period (M).[S1] Our acoustic tweezers have equal finger spacing (d) and fork finger widths (d'), which are known as uniform fork finger transducers. The intensity of the surface acoustic waves generated by IDT intensifies as the pair number (N) increases. The acoustic aperture (W) determines the width and manipulation range of TSAWs. The forked finger electrode's electrode period (M) determines the angular frequency of the forked finger electrode; the smaller the forked finger electrode width, the higher the central angular frequency.[S2]

The above main parameters have been set in order to maximize the maneuverability of tri-directional symmetrical acoustic tweezers on microparticle manipulating. As the IDTs adopted in our work are uniform forked-finger type, the finger spacing (d) and fork finger widths (d') are equal; the finger width can be calculated as

$$d=d'=M/4 \tag{S4}$$

The frequency (f') of the TSAWs generated by IDT is equal to the frequency (f) of the sinusoidal signal loaded on IDT, so it can be calculated as

$$f' = f \tag{S5}$$

The wavelength λ of the TSAWs generated by IDT can be calculated as

$$\lambda = v_s / f_0 = v_s / f \tag{S6}$$

When the frequency (f) of the sinusoidal signal loaded onto IDT is equal to the central frequency (f_0) of IDT, the excitation produces the maximum intensity of the TSAWs. Therefore the optimum finger width can be calculated using the following formulas

$$\lambda = M = v_s / f_0 \tag{S7}$$

$$d = d' = \frac{M}{4} = \frac{\lambda}{4} \tag{S8}$$

The propagation speed of TSAWs in the Z-cut $LiNbO_3$ substrate is known to be V_S = 3990 m/s, and the resonant frequency of the substrate is around 10MHz. Therefore, the wavelength of the TSAWs can be calculated to be 399 μm. And to facilitate the design of IDTs, set $\lambda = M$ = 400μm, thus the IDT was designed with a finger width and finger spacing of 100 μm.

The pair number of IDT mainly determines the intensity of TSAWs, which increases with the rise of the pair number of IDT. However, a large pair number of IDT will result in a narrow band width for the IDT, and on the other hand, the TSAWs generated by each fork finger of IDT can interfere with each other. The waveform of TSAWs can be maintained in a stable state when the pair number of IDT (N) is small, while when N is too large, TSAWs will have difficulty in maintaining a stable output and will weaken the intensity of TSAWs due to mutual interference of waves. In addition, a large pair number would make the device much difficult to fabricate. Therefore, after a comprehensive analysis, the pair number of IDT for our device was set at 50 pairs.

The acoustic aperture (W) determines the width of the TSAWs and is therefore an important parameter of IDT. The acoustic aperture is generally taken as W = (10~100)λ, because a too-small acoustic aperture W will lead to severe diffraction of the TSAWs, while a too-large acoustic aperture W will cause the equivalent capacitance of the IDTs to be too large, which is detrimental to the high-frequency signal. Therefore, the acoustic aperture W = 10mm was chosen after a comprehensive consideration.

Supplementary Figures.

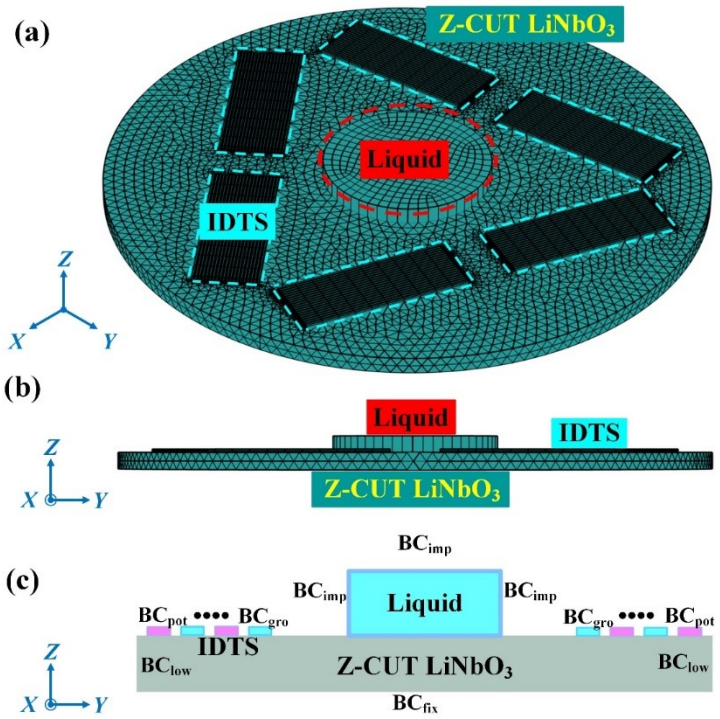

Fig. S1 The diagram of the developed numerical model with completed meshing and boundary conditions set: (a) the established numerical model includes a $LiNbO_3$ substrate layer, IDTs layer, and liquid layer. (b) The side view of the developed numerical model. (c) Schematic diagram of the setting for boundary conditions of the numerical model.

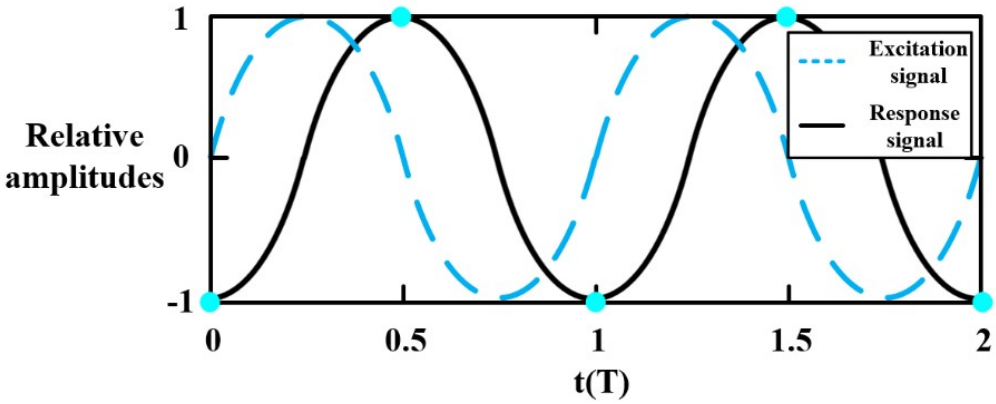

Fig.S2 Schematic representation of the calculation basis: excitation and response signals of a pair of excited IDTs; the blue dots in the diagram indicate theoretically referable calculation time points.

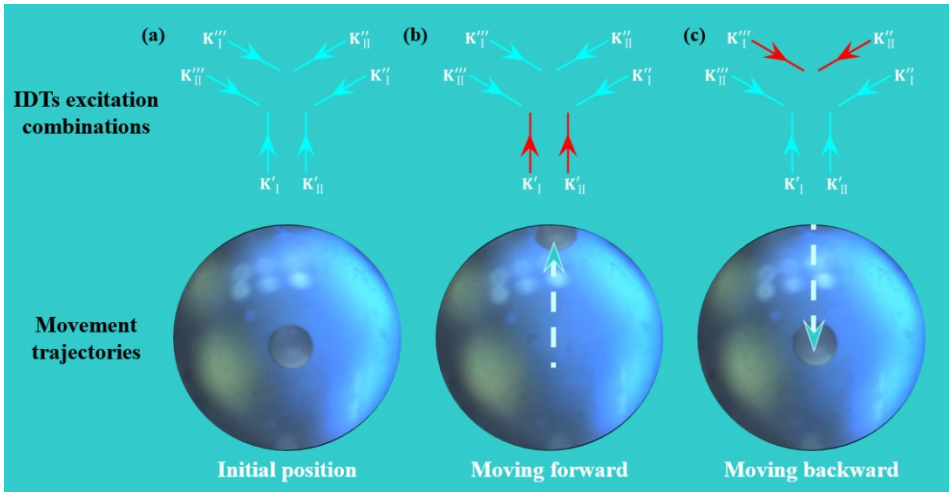

Fig.S3 Acoustic manipulation of particles reciprocating motion through different excitation combinations of IDTs. (a) IDTs off, particle located in the initial position. (b) Particle moving forward with IDTs K'_{I} and K'_{II} excited. (c) Particle moving backward with IDTs K'''_{I} and K''_{II} excited.

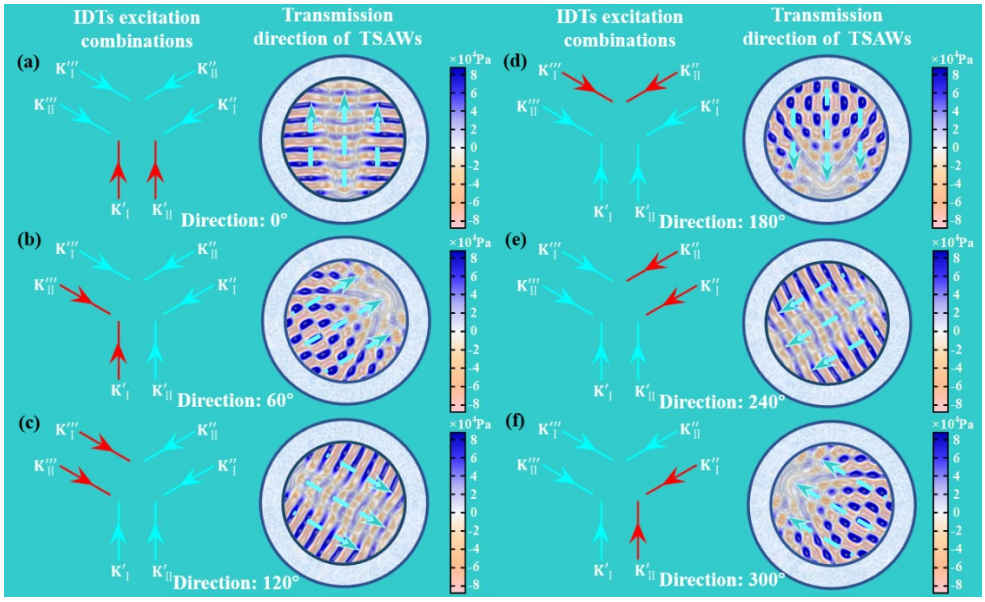

Fig.S4 Different excitation combinations of IDTs leading to various linear acoustic pressure fields and moving direction of microparticles. (a) TSAWs propagate along the 0° direction with IDTs K'_{I} and K'_{II} excited. (b) TSAWs propagate along the 60° direction with IDTs K'_{I} and K'''_{II} excited. (c) TSAWs propagate along the 120° direction with IDTs K'''_{I} and K'''_{II} excited. (d) TSAWs propagate along the 180° direction with IDTs K''_{II} and K'''_{I} excited. (e) TSAWs propagate along the 240° direction with IDTs K''_{I} and K''_{II} excited. (f) TSAWs propagate along the 300° direction with IDTs K'_{II} and K''_{I} excited.

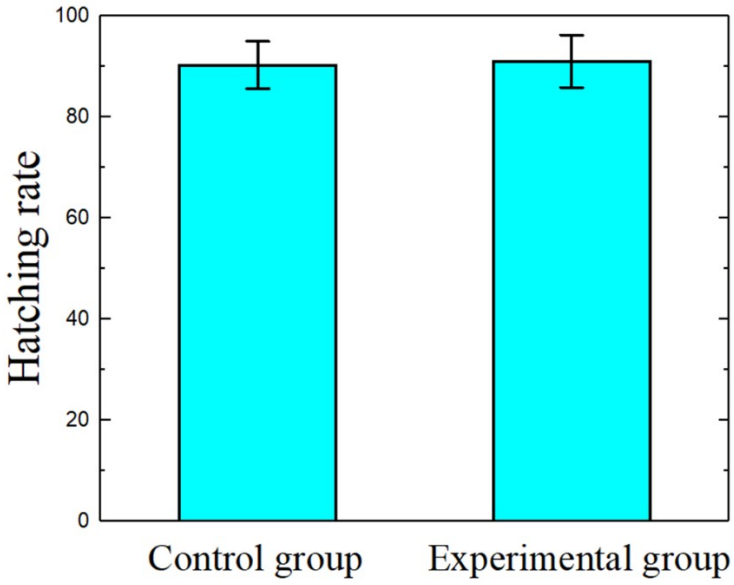

Fig.S5 The hatching rates of shrimp eggs in the controlled experiment. The eggs from the experimental group were incubated after undergoing acoustic tweezers manipulation, while the eggs from the control group were incubated without any treatment before.

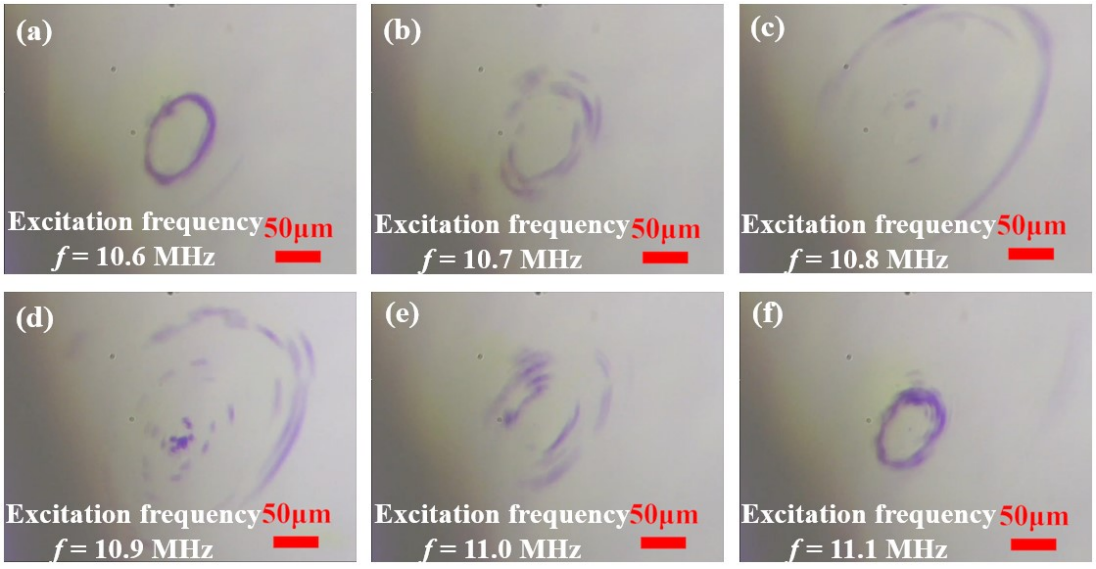

Fig.S6 The clockwise rotation trajectories of multiple microparticles with a diameter of 5μm at various excitation frequency of (a) f = 10.6MHz, (b) f = 10.6MHz, (c) f = 10.6MHz, (d) f = 10.6MHz, (e) f = 10.6MHz and (f) f = 10.6MHz.

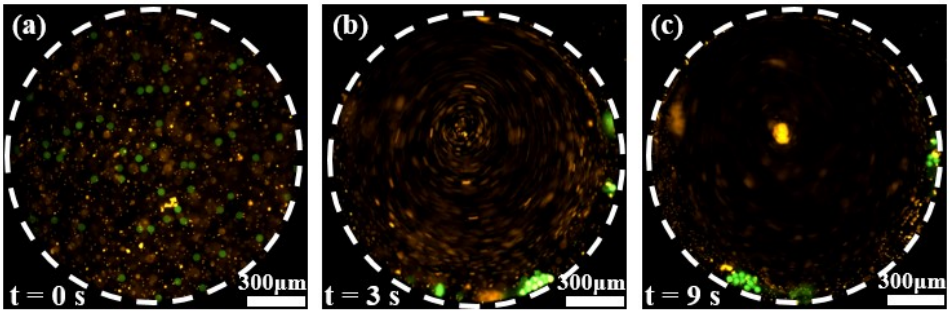

Fig.S7 The separation process of multiple microparticles with different sizes at different time (a) t = 0s, (b) t = 3s, (c) t = 9s.

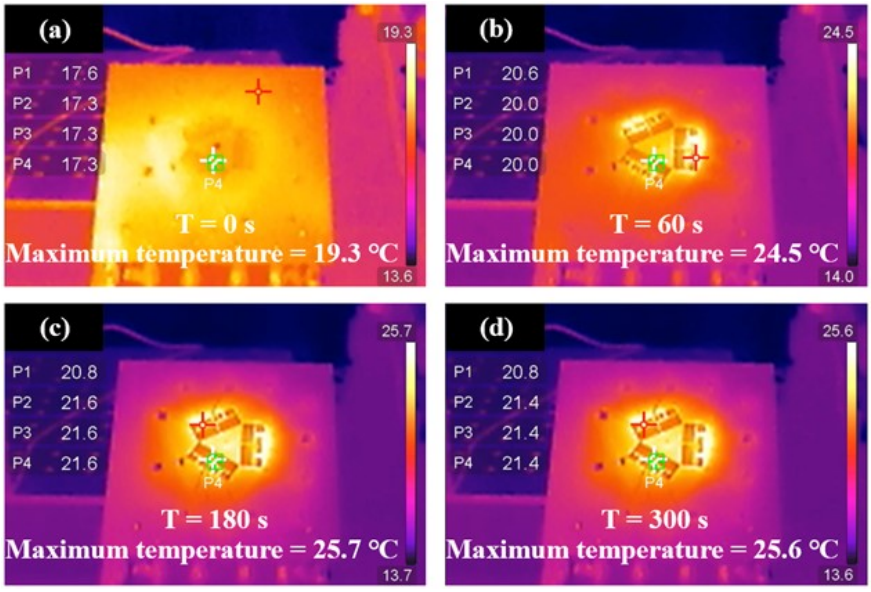

Fig.S8 The infrared holographic temperature distribution of acoustic tweezers over time.

Table S1: The detailed parameters for numerical simulation

Parameter	Symbol	Value
Density of the liquid	p_0	1-1.117 g/cm^3
Speed of TSAWs in liquid	c_0	1497 m/s
Acoustic contrast factor for polystyrene	ϕ	0.22
Wavenumber of the acoustic wave	k_y	2500 m^{-1}
Density of the microparticles	ρ_p	1.8 g/cm^3
Radius of the microparticle	a	15 μm
Dynamic viscosity of the water	η	1.43-106.17 cP
Geometry-dependent factor of the chamber	Ψ	0.4
Amplitude of substrate vibration	A	2nm
Frequency of the TSAW beams	f	10.5-11.1MHz

Supplementary Movies.

Movie S1. Linear Motion Trajectory of a Single Microparticle.

Movie S2. Clockwise Rotation Trajectory of a Single Microparticle.

Movie S3. Anticlockwise Rotation Trajectory of a Single Microparticle.

Movie S4. Manipulating the Dimer to Rotate Anticlockwise at the Center Point O of the Chamber.

Movie S5. Manipulating the Linear Trimer to Rotate Anticlockwise at the Center Point O of the Chamber.

Movie S6. Manipulating the Linear Trimer to Rotate Anticlockwise around the Center Point O of the Chamber.

Movie S7. Dynamic Conversion Process of the Triangular-shaped Trimer Rotating Anticlockwise.

Movie S8. Linear Reciprocating Motion Trajectory of a Single Biological Egg Cell.

Movie S9. Manipulating Biological Egg Cells with Acoustic Tweezers and Testing Biocompatibility.

Movie S10. Simultaneous Manipulation of Multiple Microparticles Using Tri-directional Symmetrical Acoustic Tweezers.

Movie S11. Programmable Manipulation of a Single Biological Egg Cell Using Acoustic Tweezers.

Reference

S1.T. Wang, R. Green, R. Guldiken, J. Wang, S. Mohapatra and S. S. Mohapatra, *Sensors-Basel*, 2019, **19**, 1749.

S2.L. Shu, B. Peng, C. Li, D. D. Gong, Z. B. Yang, X. Z. Liu and W. L. Zhang, *Sensors-Basel*, 2016, **16**, 526.